Dissociation Dynamics and Thermochemistry of Energy-Selected $CpCo(CO)_2^+$ Ions

Bálint Sztáray† and Tomas Baer*

Contribution from the Department of Chemistry, University of North Carolina, Chapel Hill, North Carolina 27599-3290

Received March 27, 2000

Abstract: Photoelectron photoion coincidence (PEPICO) spectroscopy has been used to investigate the dissociation dynamics of the cyclopentadienyl cobalt dicarbonyl ion, $CpCo(CO)_2^+$. The dissociation proceeds by the sequential loss of the two CO molecules. Both reactions proceed with no reverse activation energies and are slow near their dissociation onset. The 0 K onset was determined by modeling the measured dissociation rate constants with RRKM theory utilizing the variational transition state theory to locate the transition states. The ionization energy of $CpCo(CO)_2$ was measured from the threshold photoelectron spectrum to be 7.35 eV, which agrees with the literature value. The neutral $CpCo(CO)_2^+$ gas-phase heat of formation of -117 ± 10 kJ/mol was determined from the liquid value by measuring the heat of vaporization of 52.12 ± 0.68 kJ/mol. The first Co−CO bond energy in the $CpCo(CO)_2^+$ was found to be 1.53 ± 0.02 eV (148.1 ± 2 kJ/mol), giving a 298 K gas phase heat of formation of 857 ± 10 kJ/mol for $CpCoCO^+$. The second Co−CO bond energy in $CpCoCO^+$ was measured to be 1.50 ± 0.02 eV (144.8 ± 2 kJ/mol), resulting in a 298 K gas phase heat of formation of $CpCo^+$ to be 1113 ± 10 kJ/mol.

Introduction

Transition metals and transition metal complexes are used as catalysts in numerous reactions important in biology and industry. Their effectiveness depends on several factors of which the availability of metal sites that can participate in the chemical reaction is of paramount importance. The metal site becomes available when one of the ligands leaves, a process that is strongly affected by the metal ligand bond. In the case of cobalt cyclopentadienyl dicarbonyl, the two weakly bound ligands are the CO groups while the cyclopentadienyl group is strongly bound to the cobalt atom. The cobalt cyclopentadienyl dicarbonyl is the parent molecule for a host of important catalysts used for a variety of organic reactions. Substitution of pentamethyl cyclopentadienyl for the cyclopentadienyl group is a common modification since the methyl groups have an inductive effect making the cyclopentadienyl ring a better π-donor resulting in stabilization of the metal orbitals. The carbonyl ligands can also be replaced by ethylene, $H_2CCHSiMe_3$, etc. groups. These organometallic compounds have recently been used to catalyze [2+2+2] cycloaddition of diynes,[1] as well as for intramolecular hydroacylation of vinyl silanes.[2,3]

Compared to organic compounds, the heats of formation of organometallic compounds are not well established. This is in part because bomb calorimetry is not well suited for many of these molecules because the final combustion products consist of a complex mixture with the metal atom in various and not easily predicted oxidation states.[4,5] For instance in the case of cyclopentadienyl cobalt dicarbonyl ($CpCo(CO)_2$), the combustion products consisted of 22% Co_3O_4, 56% CoO, and 22% Co.[6] The available thermochemical data on organometallic complexes come in a variety of forms. Much of the thermochemistry for neutral compounds refers to the condensed phase,[7,8] while most of the bond energy information on ions refers to the gas phase.[7,9−11] An exception is the reported enthalpies of protonation that have been measured for a wide range of organometallic compounds in solution by Angelici.[12] The condensed-phase heat of formation of cyclopentadienyl−cobalt−dicarbonyl has been measured by static bomb calorimetry by Chipperfield et al.[6] However, no gas-phase data are available. These are needed in the present study for the determination of the $\Delta_f H°$ of the $CpCo(CO)_2^+$ ion and its fragments.

In this study we report on the investigation of the gas-phase ionic properties of $CpCo(CO)_2^+$ by the technique of photoelectron photoion coincidence (PEPICO), a method for energy selecting ions and determining their dissociation rate constants.

† Present address: Department of General and Inorganic Chemistry, Eötvös Loránd University, Budapest, Hungary.

(1) Boese, R.; van Sickle, A. P.; Vollhardt, K. P. *Synthesis* **1994**, 1374−1382.
(2) Lenges, C. P.; Brookhart, M.; Grant, B. E. *J. Organomet. Chem.* **1997**, *528*, 199−203.
(3) Lenges, C. P.; White, P. S.; Brookhart, M. *J. Am. Chem. Soc.* **1998**, *120*, 6965−6979.
(4) Cox, J. D.; Pilcher, G. *Thermochemistry of organic and organometallic compounds*; Academic Press: London, 1970.
(5) Pilcher, G. Combustion calorimetry of organometallic compounds. In *Energetics of Organometallic Species*; Martinho Simões, J. A., Ed.; Kluwer Academic Publ.: Dordrecht, The Netherlands, 1992; pp 9−34.
(6) Chipperfield, J. R.; Sneyd, J. C. R.; Webster, D. E. *J. Organomet. Chem.* **1979**, *178*, 177−189.
(7) Martinho Simões, J. A.; Beauchamp, J. L. *Chem. Rev.* **1990**, *90*, 629−688.
(8) Nolan, S. P. Bonding energetics of organometallic compounds. In *Encyclopedia of Inorganic Chemistry*; King, R. B., Ed.; Wiley: New York, 1994; pp 307−318.
(9) Beauchamp, J. L.; van Koppen, P. A. M. Fundamental gas-phase studies of the mechanism and thermochemistry of organometallic reactions. In *Energetics of Organometallic Species*; Martinho Simões, J. A., Ed.; Kluwer Academic Publ.: Dordrecht, The Netherlands, 1992; pp 287−320.
(10) Meyer, F.; Armentrout, P. B. *Mol. Phys.* **1996**, *88*, 187−197.
(11) Haynes, C. L.; Fisher, E. R.; Armentrout, P. B. *J. Am. Chem. Soc.* **1996**, *118*, 3269−3280.
(12) Angelici, R. J. *Acc. Chem. Res.* **1995**, *28*, 51−60.

10.1021/ja001077q CCC: $19.00
Published on Web 09/09/2000

When these results are analyzed with the statistical theory of unimolecular reactions, it is possible to extract accurate dissociation limits and thus bond energies. This thermochemical information can be used in conjunction with the ionization energy of CpCoCO to determine the Co−CO bond energy of the neutral $CpCo(CO)_2$. The determination of this latter quantity is planned in future experiments.

Experimental Approach

Cyclopentadienyl−cobalt−dicarbonyl ($CpCo(CO)_2$, min 95% purity) was purchased from *Strem Chemicals* and was used without further purification. Traces of the dimer ($C_{10}H_{12}$: 4,7-methano-3a,4,7,7a-tetrahydro-1*H*-indene) of the presumed starting compound and cyclopentadiene (C_5H_6) were detected in the time-of-flight mass spectra. Because these mass peaks did not coincide with any of the $CpCo(CO)_2$ parent or daughter ion signals, they had no influence on the measurements.

The threshold photoelectron photoion coincidence (TPEPICO) apparatus has been described previously.[13,14] Briefly, the room temperature sample molecules were ionized with vacuum ultraviolet (VUV) light from an H_2 discharge lamp dispersed by a 1 m normal incidence monochromator. The VUV wavelengths were calibrated using the hydrogen Lyman-α line. The ions and the electrons were extracted in opposite directions with an electric field of 20 V/cm. Threshold photoelectrons were selected by a steradiancy analyzer that consists of a flight tube with small apertures that stops energetic electrons. Further discrimination against the energetic electrons was provided by a hemispherical electrostatic sector analyzer resulting in a ~35 meV combined photon and electron energy resolution. After exiting the 5 cm long first acceleration region, the ions entered a second (0.5 cm) acceleration region in which they were accelerated to 210 eV and were detected after drifting through a 32 cm field-free drift region. The electrons and ions were detected with a channeltron electron multiplier and a multichannel plate detector, respectively. The electron and ion signals served as start and stop pulses for measuring the ion time-of-flight (TOF), and the TOF for each coincidence event was stored on a multichannel pulse height analyzer. TOF distributions were obtained in 1 to 72 h depending on the photon intensity and the desired spectrum quality.

The PEPICO spectra were used for two purposes. First, the fractional abundances of the parent and the daughter ions were measured as a function of the photon energy. Second, because slowly dissociating (metastable) ions decay while traversing the 5 cm acceleration region, the daughter ion TOF distribution is asymmetric, an asymmetry that can be analyzed to extract the ion decay rates as a function of ion internal energy. These two types of information were used together in the data analysis.

Experimental Results

TPEPICO Measurements. TOF mass spectra of $CpCo(CO)_2$ were collected in the photon energy range of 8.84−11.11 eV. Typical time-of-flight distributions are shown in Figure 1a,b. The experimental data are plotted as points while the solid line shows the fitted TOF distributions as discussed in the data analysis section. Below a photon energy of 10 eV the two peaks correspond to the molecular ion, $CpCo(CO)_2^+$, and its daughter ion, $CpCoCO^+$. At photon energies in excess of 10.5 eV, the two peaks are from $CpCoCO^+$ and $CpCo^+$. Since the maximum available photon energy in the instrument is about 13.5 eV, no cyclopentadienyl loss is observable. According to the literature, the appearance energy of the cobalt ion is above 16 eV.[15] As shown in Figure 1, in the case of both the first and the second carbonyl losses, the daughter ion TOF distributions are asymmetric at energies close to the appearance energy of these fragments. This indicates that the ions dissociate during the course of acceleration in the first acceleration region of the ion analyzer. If their average lifetime is comparable to the time it takes to traverse the acceleration regions (~9.6 μs) then the

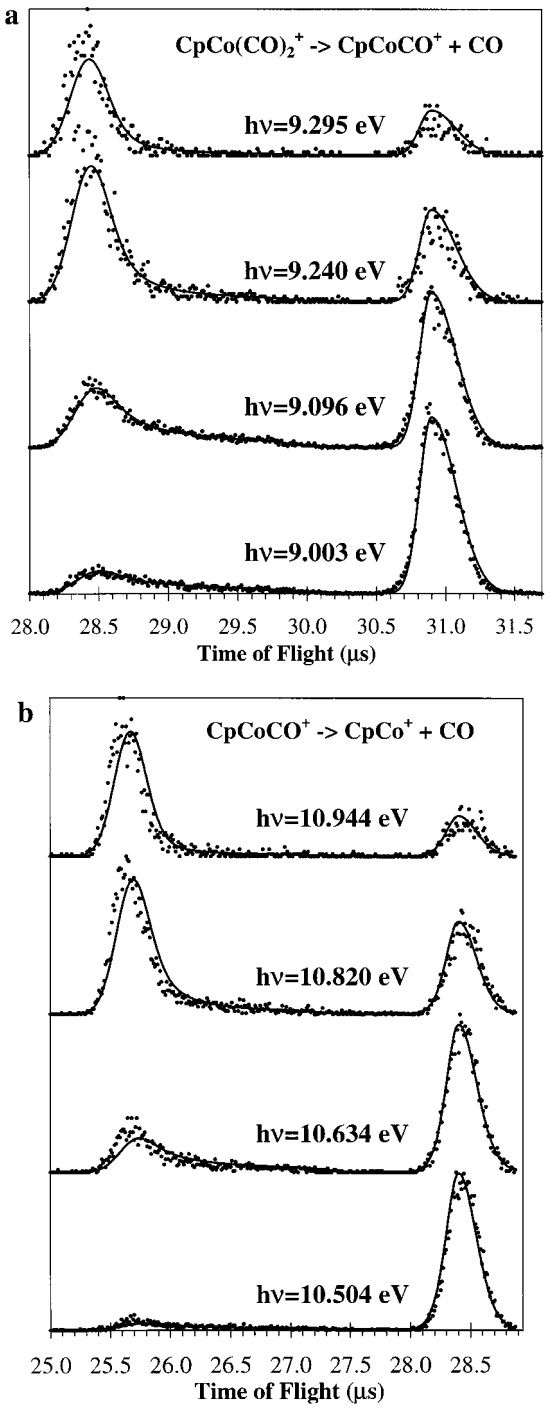

Figure 1. Ion TOF distributions at selected photon energies. Points are the experimental data, while the solid lines show the calculated TOF distributions. (a) The first carbonyl loss: the asymmetric peak between 28.5 and 30 μs is assigned to the $CpCoCO^+$ ion, while the symmetric peak at 31 μs is due to the parent ion, $CpCo(CO)_2^+$. (b) The second carbonyl loss: the asymmetric peak around 25.5−27 μs corresponds to the $CpCo^+$ ion, while the symmetric peak at 28.5 μs is due to the first daughter ion, $CpCoCO^+$.

(13) Baer, T.; Booze, J. A.; Weitzel, K. M. Photoelectron photoion coincidence studies of ion dissociation dynamics. In *Vacuum ultraviolet photoionization and photodissociation of molecules and clusters*; Ng, C. Y., Ed.; World Scientific: Singapore, 1991; pp 259−298.

(14) Keister, J. W.; Baer, T.; Evans, M.; Ng, C. Y.; Hsu, C. W. *J. Phys. Chem.* **1997**, *101*, 1866−1872.

(15) Rosenstock, H. M.; Draxl, K.; Steiner, B. W.; Herron, J. T. *J. Phys. Chem. Ref. Data* **1977**, *6*.

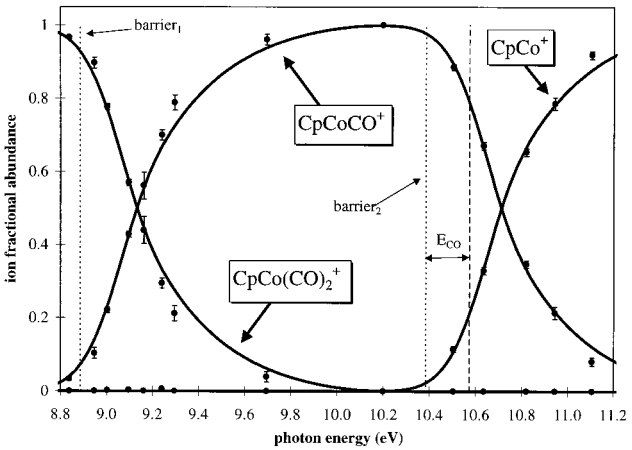

Figure 2. Breakdown curves of the two consecutive carbonyl-loss steps. The points are the experimental data with error estimates. Solid lines are the simulation results using RRKM theory and convolution with the thermal energy distribution.

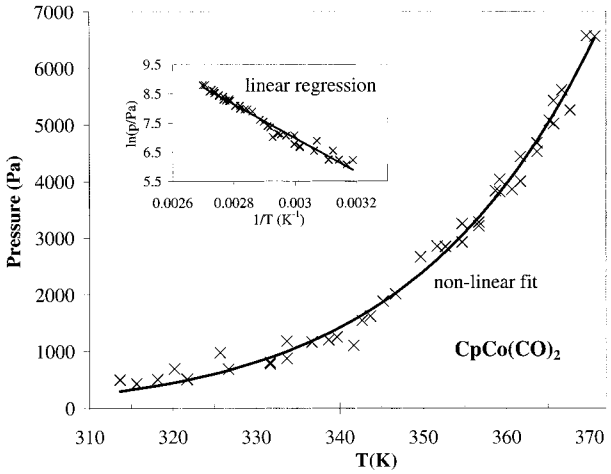

Figure 3. The vapor pressure of $CpCo(CO)_2$ in the range of 310−370 K. The solid curve is a result of a nonlinear fit to the experimental data (crosses). The box shows a linear regression plot whose slope is $\Delta H_{vap}/R$.

time-of-flight of the fragment ion is between the parent and daughter ion TOF, and a quasiexponential shape is observed in the daughter-ion peak. The decay rate can be determined from the analysis of the peak shapes. Those ions that dissociate after exiting the first acceleration region are counted as parent ions. In slow reactions this relatively short time scale of the PEPICO experiment leads to the so-called kinetic shift.[16] That is, the observed dissociation onset does not correspond to the true dissociation energy, but is shifted to an energy at which the dissociation rate constant is sufficiently large to permit ions to dissociate in the acceleration region.

Figure 2 shows the breakdown diagram of the $CpCo(CO)_2^+$ ion in which the ion fractional abundance is plotted as a function of the photon energy. The points are the experimental ratios with error estimates, while the solid lines show the simulation results. The broken lines indicate the location of the two dissociation barriers and the energy carried away by the first CO molecule as discussed in the following sections.

Vapor Pressure Measurement. To calculate the gas-phase heat of formation of $CpCo(CO)_2$ from the condensed-phase data,[6] its heat of vaporization was measured. A vapor pressure measurement apparatus was assembled from a flask, a mercury U-tube, a thermometer, and mechanical vacuum pump. Since $CpCo(CO)_2$ is air-sensitive, sample handling was performed in an argon glovebox. The vapor pressure was determined in a temperature range between room temperature and the boiling point of water, which was used as a heat bath. The vapor pressure data are plotted in Figure 3 as points while the solid lines are the fitted curves according to the Clausius−Clapeyron equation, where C is a constant:

$$\ln P_v = \frac{-\Delta H_{vap}}{RT} + C \qquad (1)$$

The heat of vaporization was determined to be 52.12 ± 0.68 kJ/mol. Because the error in the condensed phase heat of formation ($-169. \pm 10$ kJ/mol) is significantly larger than the error introduced here, the accuracy of the gas-phase heat of formation is determined by the original liquid-phase heat of combustion measurement. The suggested value of the gas-phase heat of formation of $CpCo(CO)_2$ is -117 ± 10 kJ/mol.

Data Analysis. The extraction of thermochemical data and bond energies from the experiment requires a careful analysis of rates in terms of the ion energy distribution. Although the TPEPICO resolution is about 35 meV, the thermal energy distribution of the $CpCo(CO)_2$ extends from 0 to 0.4 eV. To properly model the two consecutive reactions it is necessary to interpret the measured rate constants in terms of a distribution of $k(E)$ in which the energy extends over this thermal energy distribution. The reaction mechanism (eq 2) for excited ions involves a sequential loss of the two CO groups.

$$CpCo(CO)_2 \rightarrow CpCo(CO)_2^+ \rightarrow \underset{+\,CO}{CpCoCO^+} \rightarrow \underset{+\,CO}{CpCo^+} \qquad (2)$$

The first step of the analysis is the calculation of the thermal energy distribution of the neutral cyclopentadienyl−cobalt−dicarbonyl using the usual relation:

$$P(E) = \frac{\rho(E)e^{-E/RT}}{\int_0^\infty \rho(E)e^{-E/RT}\,dE} \qquad (3)$$

in which $\rho(E)$ is the rovibrational density of states calculated using a direct count method.[17,18] The molecule was approximated as a symmetric top by replacing the experimental rotational constants ($A = 1625$ MHz, $B = 1257$ MHz, $C = 876$ MHz)[19] with the geometric average of the A and B (1429 MHz). The harmonic frequencies of the neutral species were calculated using density functional theory with B3LYP functional[20,21] and the pvdz basis set of Ahlrichs and co-wokers,[22] and scaled with a factor of 0.95 to get good agreement with the infrared spectra in the literature.[23] The calculated frequencies are given in Table 1. The lowest frequency mode, namely the cyclopentadienyl ring rotation, was not treated as a vibration because the experimentally determined barrier height[19] of 27 cm^{-1} corresponding to this motion is just twice the zero-point energy of

(16) Chupka, W. A. *J. Chem. Phys.* **1959**, *30*, 191−211.
(17) Beyer, T.; Swinehart, D. R. *ACM Commun.* **1973**, *16*, 379.
(18) Baer, T.; Hase, W. L. *Unimolecular Reaction Dynamics: Theory and Experiments*; Oxford University Press: New York, 1996.
(19) Roehrig, M. A.; Chen, Q. Q.; Haubrich, S. T.; Kukolich, S. G. *Chem. Phys. Lett.* **1991**, *183*, 84−88.
(20) Becke, A. D. *J. Chem. Phys.* **1992**, *97*, 9173.
(21) Lee, C.; Yang, W.; Parr, R. G. *Phys. Rev.* **1988**, *B37*, 785−789.
(22) Schäfer, A.; Horn, H.; Ahlrichs, R. *J. Chem. Phys.* **1992**, *97*, 2571−2577.
(23) Crichton, O.; Rest, A. J.; Taylor, D. J. *J. Chem. Soc. Dalton Trans.* **1980**, 167−173.

Table 1. The Vibrational Frequencies of Relevant Species[a]

CpCo-$(CO)_2$	CpCo-$(CO)_2^+$	CpCo-$CO\cdots CO^+$	CpCo-CO^+	$CpCo\cdots CO^+$	$CpCo^+$
7	*46*	*−35*[b]	*60*	*−26*[b]	220
95	87	*11*	97	*9*	295
101	105	13	240	11	328
111	109	49	281	44	345
300	277	52	314	46	515
310	301	52	349	216	671
323	319	79	393	295	784
347	332	241	421	328	787
441	367	281	494	346	798
476	411	315	526	517	845
510	423	348	745	669	891
526	440	393	789	784	892
565	497	422	802	787	938
573	536	495	805	798	952
594	555	527	872	845	981
760	785	746	905	891	987
772	797	789	912	893	1069
799	812	802	929	939	1212
803	821	805	982	952	1217
837	886	871	1000	980	1297
881	919	904	1003	988	1353
890	928	912	1075	1070	1398
950	940	929	1219	1210	3067
981	985	983	1272	1217	3067
1009	1014	1000	1313	1296	3076
1009	1015	1003	1377	1355	3084
1084	1081	1075	1417	1398	3090
1214	1220	1219	2130	2154	
1326	1305	1273	3063	3066	
1339	1341	1313	3075	3067	
1373	1374	1378	3081	3075	
1415	1431	1417	3087	3083	
1989	2121	2130	3093	3090	
2034	2146	2152			
3071	3073	3063			
3071	3076	3075			
3082	3083	3080			
3090	3086	3086			
3097	3095	3093			

[a] The equilibrium species are from DFT(B3LYP) calculations. The transition state frequencies are from DFT(B3LYP) calculations except for the lowest 3 or 4 frequencies that were fitted to the experiment. [b] Reaction coordinate

this mode. The density of states for this internal degree of freedom was calculated as a hindered (Pitzer) rotor[18,24] using the experimental barrier height of 820 GHz (27 cm^{-1}) and the ab initio calculated lowest frequency. The moment of inertia of the hindered rotor was obtained from the reduced moment of the two parts of the molecule. The moment of inertia of the cyclopentadienyl ring was taken from the electron-diffraction experiment,[25] while the other moment used was simply $h^2/2A$ obtained from the microwave measurement.[19] The density of states, $\rho(E)$, in eq 3 was calculated by starting with the $\rho_r(E)$ for the three molecular rotors (symmetric top), convoluting this with the density of the Pitzer rotor, and then finally using this as the starting vector in the direct-count of the density of states of the remaining vibrational degrees of freedom. Figure 4 shows the thermal energy distribution of the sample at 298 K.

The thermal energy distribution of the neutral $CpCo(CO)_2$ was calculated to obtain the energy distribution of the first ion. The latter is represented by a convolution of the electron energy analyzer function with the thermal energy distribution of the neutral. The analyzer function can be measured from a threshold photoelectron (TPES) spectrum of a rare gas, NO, or acetylene.

(24) Pitzer, K. S. *Quantum Chemistry*; Prentice Hall: New York, 1953.
(25) Beagley, B.; Parrott, C. T.; Ulbrecht, V.; Young, G. G. *J. Mol. Struct.* **1979**, *52*, 47−52.

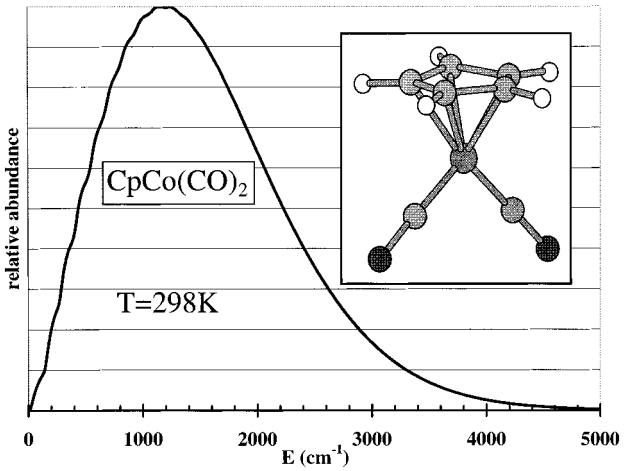

Figure 4. Calculated thermal distribution of the $CpCo(CO)_2$ internal energy at a temperature of 298 K.

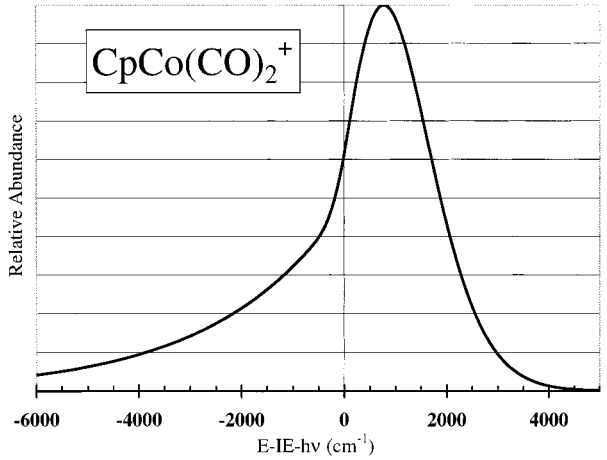

Figure 5. Calculated internal energy distribution of the $CpCo(CO)_2^+$ ion. This is a convolution of the thermal energy distribution and the electron energy resolution function. The long tail to negative energies is due to hot electrons.

Figure 5 shows the convolution of this analyzer function with the thermal energy distribution (eq 3). Zero energy on the plot corresponds to the photon energy minus the adiabatic ionization energy.

The energy distribution of the second ion, $CpCoCO^+$, is somewhat more complicated to determine. After $CpCo(CO)_2^+$ ions of a particular internal energy, E, dissociate, they leave behind $CpCoCO^+$ product ions in a distribution of internal energies from 0 to $E - E_o$. We can determine their average internal energy using the Klots equation:[26]

$$E - E_0 = E_{tr} + E_{ro}(CO) + E_v(CO) + E_{ro}(CpCoCO^+) + E_v(CpCoCO^+)$$

$$= kT^* + kT^* + 0 + \frac{3}{2}kT^* + \sum_{i=1}^{s}\frac{h\nu_i}{e^{h\nu_i/kT^*} - 1} \qquad (4)$$

This equation assumes, in the spirit of the statistical theory, that the various modes (vibrational, rotational, and translational) of the dissociating system are in thermal equilibrium with each other. It is quite reliable for systems that dissociate without a barrier,[18] as is the case for the reactions discussed in this paper. By solving this equation for the common temperature, T^*, that

(26) Klots, C. E. *J. Chem. Phys.* **1973**, *58*, 5364−5367.

defines a statistical system, the average rotational and vibrational energy remaining in the $CpCoCo^+$ ion can be obtained. In eq 4 the translational energy is kT^* (2 degrees of freedom according to the phase space theory).[27] Although the bulk of the excess energy is deposited in the $CpCoCO^+$ fragment ion as vibrational and rotational energy, a significant amount of energy is taken away as translational, as well as rotational, energy of the CO product. By carrying out the above procedure for each energy in the parent ion internal energy distribution, the energy distribution of the second ion can be obtained.

Rate Constant Determination and Breakdown Diagram. Rate constants were calculated for the two unimolecular dissociation steps of the $CpCo(CO)_2^+$ ion. RRKM calculations were performed using the well-known formula:[18,28−30]

$$k(E) = \frac{\sigma N^{\#}(E - E_0)}{h\rho(E)} \quad (5)$$

in which $N^{\#}(E - E_0)$ is the sum of states of the transition state from 0 to $E - E_0$ and $\rho(E)$ is the density of states of the ion measured from the bottom of the ion ground-state potential energy well. The symmetry parameter, σ, is 2 in the first dissociation and 1 in the second. The vibrational frequencies were calculated at the B3LYP/pvdz (DFT) level of theory for the ions and the transition states. These frequencies were scaled with the previously mentioned factor of 0.95. Details about the calculation and the location of the transition states are given in a following section of this paper.

The ion TOF distribution and the breakdown diagram can be calculated using the following information: the thermal energy distribution, the ionization energy, and the acceleration electric fields and the acceleration and drift distances. In addition, the ionization energy of the $CpCo(CO)_2$ was fixed at 7.35 eV, a PES value[31] that was confirmed by our threshold PES measurement. The following variable parameters were adjusted until a best fit was obtained: the dissociation limits, the lowest three or four TS vibrational frequencies (not counting the frequency associated with the Cp-ring rotation, since it was treated as a hindered rotor), and to a limited extent the threshold electron analyzer function. This calculation described by Keister et al.[32] was used to extract the dissociation limits. The best fit was found by minimizing the following function:

$$\mathrm{Err} = 1 - \frac{\langle E|S\rangle}{\sqrt{\langle E|E\rangle\langle S|S\rangle}} = 1 - \frac{\sum_i E_i S_i}{\sqrt{\sum_i E_i E_i \sum_i S_i S_i}} \quad (6)$$

where E_i and S_i are the experimental and simulated points for either the TOF distribution or the breakdown diagram. This Err function varies from 1 to 0, the latter value corresponding to a perfect fit in which S and E are equal.

The best fit to both the TOF distributions and the breakdown diagram was obtained with the following parameters: $\mathrm{barrier}_1 = 12378\ \mathrm{cm}^{-1}$, $\mathrm{barrier}_2 = 12088\ \mathrm{cm}^{-1}$, TS_1 lowest frequencies 13, 49, 52, and 52 cm^{-1}, and TS_2 frequencies 11, 44, and 46 cm^{-1}. The simulated breakdown curves for the two dissociations and the simulated TOF distributions are shown in the figures mentioned above. The RRKM calculated rate constants are plotted in Figure 6. The vibrational frequencies allow us to calculate a canonical $\Delta S^{\#}$ at some arbitrary temperature. At 1000 K, the entropy of activations for the two reactions were 62 and 58 J/(mol K). These are characteristic of very loose transition states.

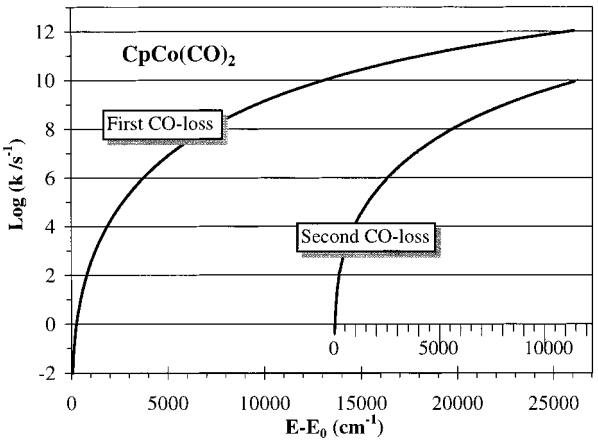

Figure 6. The RRKM calculated rate constants. Note that the energy scale is different for the two curves. The origin of the second axis is not at the barrier height of the second dissociation, rather it is that excess energy after the first carbonyl loss, where the remaining energy of the $CpCoCO^+$ fragment in the product energy distribution is equal to the second barrier.

The uncertainties in the derived parameters were also studied. Calculations for fitting the TOF distributions and the breakdown curve with fixed transition state frequencies were carried out studying the effect of altering these frequencies with a factor, thus simulating a looser or tighter TS. The quality of the fit, i.e., the calculated Err function in eq 5, for the breakdown curve changed only slightly when the lowest frequencies were modified by 20% or 40%. As a result of this frequency change, the optimized barrier heights were shifted by approximately 0.04−0.05 eV. However, the quality of the calculated TOF distributions was significantly worse: a 20% increase in the lowest frequencies caused a 40−150% increase in the error of the TOF distributions. In the worst case, the error increased from 0.0057 to 0.014. These findings indicate the importance of the rate studies in determining reliable onsets.

The derived barriers correspond to dissociative photoionization limits of 8.88 ± 0.02 and 10.38 ± 0.02 eV for the loss of one and two CO groups, respectively. These can be compared to the literature values based on nonmonochromatic electron impact measurements 10.1 ± 0.2 and 11.7 ± 0.2 eV.[33] Using monochromatic electrons, Pignataro and Lossing reported the onset for the loss of two CO groups as 10.8 ± 0.2 eV.[34] The first measurement suffered from poor energy resolution of the electron impact method, the unfavorable threshold law for electron impact that results in an ionization cross section that is vanishingly small at threshold, and ignoring the kinetic shift. The Pignataro and Lossing experiment was limited mainly for the latter two reasons.

The effect of the thermal energy and the slow rate constants for the first CO loss channel are shown in Figure 7. If the sample were at 0 K, the electron energy resolution infinitely good, and

(27) Light, J. C. *J. Chem. Phys.* **1964**, *40*, 3221−3229.
(28) Kassel, L. S. *J. Phys. Chem.* **1928**, *32*, 225−242.
(29) Marcus, R. A.; Rice, O. K. *J. Phys. Colloid Chem.* **1951**, *55*, 894−908.
(30) Rice, O. K.; Ramsperger, H. C. *J. Am. Chem. Soc.* **1927**, *49*, 1617−1629.
(31) Lichtenberger, D. L.; Calabro, D. C.; Kellogg, G. E. *Organometallics* **1984**, *3*, 1623.
(32) Keister, J. W.; Baer, T.; Thissen, R.; Alcaraz, C.; Dutuit, O.; Audier, H.; Troude, V. *J. Phys. Chem. A* **1998**, *102*, 1090−1097.
(33) Winters, R. E.; Kiser, R. W. *J. Organomet. Chem.* **1965**, *4*, 190.
(34) Pignataro, S.; Lossing, F. P. *J. Organomet. Chem.* **1968**, *11*, 571−576.

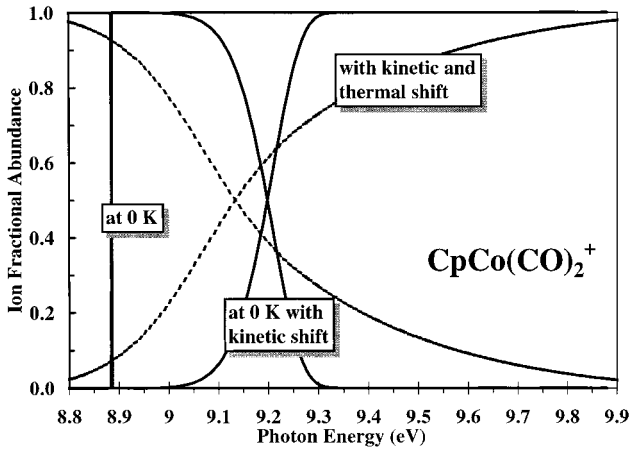

Figure 7. Simulated breakdown curves for the first CO loss showing the thermal and kinetic effects. The sharp stepped curve at 8.88 eV is the expected 0 K breakdown diagram if the reaction were infinitely fast, the energy resolution perfect, and the sample internally cold at 0 K. Thus, each parent ion with an internal energy higher than the barrier height will dissociate. The breakdown curve with the highest energy crossover energy at 9.2 eV (solid lines) shows the effect of the finite measurement time (6.9 μs) and the slow rate constant, so that only parent ions with sufficient energy above the barrier dissociate in the acceleration region. The third curve, shown as a dashed line with an intermediate crossover, corresponds to the real measurement conditions that include the thermal energy distribution of the neutral species, the finite energy resolution of our instrument, and the measured rate constant as a function of ion internal energy. The dashed line is also plotted in Figure 2.

the rate constant fast at the thermochemical dissociation limit, the breakdown diagram would have the form of a step function located at the 0 K dissociation limit of 8.88 eV. The effect of the slow dissociation rate shifts the crossover energy to about 9.20 eV. At this energy (2600 cm^{-1} above the dissociation limit) the rate constant according to Figure 6 has reached at about 10^5 s^{-1}. If the thermal energy is convoluted into this simulation, the cross over energy shifts back down to 9.13 eV and the shape of the breakdown diagram broadens out.

Quantum Chemical and VTST Calculations. To carry out the RRKM simulation of the experimental data, reliable equilibrium and transition state frequencies are required. Since ion and especially transition state frequencies are not easily available from measurements, we calculated these with density functional theory (DFT).[35]

The neutral $CpCo(CO)_2$ and ion energies and structures were calculated with the B3LYP functional[21] using pvdz and pvtz basis sets[22] available within the Gaussian 98 system of programs.[36] To reduce computation costs, the molecule was assumed to have C_s symmetry. The most important features of the calculated geometries for the neutral and its ion are compared with the experimental values for the neutral $CpCo(CO)_2$ in Table 2. The neutral molecule was calculated at several levels of theory. The Hartree−Fock results were not very good and are not shown in the table. However, the many-body perturbation theory (MBPT(2))[37] and B3LYP results are comparable in accuracy, with the latter one being computationally much less demanding.

The CO loss reaction from organometallic complexes proceeds with no barrier in the exit channel, which causes difficulties in establishing the structure of the transition state. We thus located the transition state using variational transition state theory (VTST),[18,38,39] according to which the TS is located at a Co−CO bond distance that corresponds to a minimum in the sum of states. This means that vibrational frequencies need to be calculated as a function of the Cp−CO bond distance. Accordingly, one of the two cobalt−carbonyl distances was fixed at values from the equilibrium distance to 6.0 Å, while all the other coordinates were optimized. The vibrational frequencies were calculated in all of these quasioptimized structures, which resulted in real frequencies except for the one imaginary frequency (the cobalt−carbonyl stretch). Since these quasioptimized structures are not stationary points on the potential energy surface, the calculation of the vibrational frequencies is not straightforward, and one has several choices how to incorporate the remaining forces.[40] In our case, the frequencies were calculated by diagonalizing the analytic Hessian, neglecting the forces. This is the simplest possible choice, and in this case the error introduced here would probably not bias the qualitative results concerning the trends in the frequencies and the approximate location of the phase-space bottleneck. Figure 8 shows what happens to the lowest 12 frequencies. It is obvious that the sixth frequency (*F*), which is the reaction coordinate Cp−CO stretch, goes imaginary beyond the inflection point of the potential energy curve. The eighth (*H*) and the ninth (*I*) frequencies go down significantly along the reaction coordinate, since they correspond to the rotations of the carbon monoxide in the dissociation limit. Two other coordinates (*A* and *B*) that eventually end up as free rotations decrease as well to values below 10 cm^{-1}. They correspond to the two scissoring vibrations of the carbonyls. A final vibration (*C*) that is strongly affected but remains a vibration after dissociation is associated with the Cp-ring.

These frequency curves were used to locate the transition state using variational transition state theory.[18,38,39] The sum of states was calculated with each of the frequency sets at several energies above the dissociation limit. The sum of states, $N^{\#}[E - E_{PE}(r)]$, shown in Figure 9 was calculated over the energy range from 0 to $E - E_{PE}(r)$, where E is the ion energy and $E_{PE}(r)$ is the value of the potential energy function at the particular r(Co−CO). Because the internal energy is monotonically decreasing while the vibrational frequencies are monotonically decreasing along the reaction coordinate, a minimum in the sum of states (the reaction bottleneck) should appear at some internuclear distance. At the lowest two ion energies shown in Figure 9, the minimum lies at a very large r(Co−CO) bond distance. However, at the highest energy shown in Figure 9, the minimum has moved in so that a very shallow minumum is evident around 4.5 Å. However, all the sum curves are quite flat in this region indicating that this reaction proceeds via a loose transition state with no well-defined location for the transition state. Because the interesting region of the dissociation

(35) Parr, R. G.; Yang, W. *Density Functional Theory of Atoms and Molecules*; Oxford University Press: New York, 1989.

(36) Frisch, M. J.; Trucks, G. W.; Schlegel, H. B.; Scuseria, G. E.; Robb, M. A.; Cheeseman, J. R.; Zakrzewski, V. G.; Montgomery, J. A.; Stratmann, R. E.; Burant, J. C.; Dapprich, S.; Millam, J. M.; Daniels, A. D.; Kudin, K. N.; Strain, M. C.; Farkas, Ö.; Tomasi, J.; Barone, V.; Cossi, M.; Cammi, R.; Mennucci, B.; Pomelli, C.; Adamo, C.; Clifford, S.; Ochterski, J.; Petersson, G. A.; Ayala, P. Y.; Cui, Q.; Morokuma, K.; Malick, D. K.; Rabuck, A. D.; Raghavachari, K.; Foresman, J. B.; Cioslowski, J.; Ortiz, J. V.; Baboul, A. G.; Stefanov, B. B.; Liu, G.; Liashenko, A.; Piskorz, P.; Komáromi, I.; Gomperts, R.; Martin, R. L.; Fox, D. J.; Keith, T.; Al-Laham, M. A.; Peng, C. Y.; Nanayakkara, A.; Gonzalez, C.; Challacombe, M.; Gill, P. M. W.; Johnson, B. G.; Chen, W.; Wong, M. W.; Andres, J. L.; Head-Gordon, M.; Replogle, E. S.; Pople, J. A. GAUSSIAN 98, Revision A.7, Gaussian, Inc.: Pittsburgh, PA, 1998; Ref Type: Computer Program.

(37) Bartlett, R. J. *Annu. Rev. Phys. Chem.* **1981**, *32*, 359.

(38) Hase, W. L. *Chem. Phys. Lett.* **1987**, *139*, 389−394.

(39) Wardlaw, D. M.; Marcus, R. A. *Adv. Chem. Phys.* **1988**, *70*, 231−263.

(40) Allen, W. D.; Császár, A. G. *J. Chem. Phys.* **1993**, *98*, 2983−3015.

Table 2. Calculated and Experimental Geometrical Parameters of $CpCo(CO)_2$ and Its Ion

		MBPT(2)-neutral		DFT (B3LYP)-neutral		DFT(B3LYP)-ion
	expt[a]	pvdz	pvtz	pvtz	pvdz	pvdz
r(CC) (Å)[b]	1.450(3)	1.436	1.431	1.423	1.428	1.430
r(CH) (Å)[b]	1.083 (fixed)	1.088	1.077	1.078	1.089	1.090
r(Co−C) (Å)[b]	2.129(6)	2.014	2.004	2.129	2.127	2.147
r(Co−CO) (Å)	1.679(4)	1.618	1.610	1.749	1.746	1.851
r(CO) (Å)	1.191(4)	1.176	1.176	1.146	1.150	1.129
a(CCoC) (deg)	98.4(8)	90.33	89.65	93.56	94.11	100.19
a(OCCo) (deg)	180 (fixed)	179.65	178.79	179.39	179.04	178.53
t(CCoCO) (deg)		53.58	13.46	156.56	165.01	124.02

[a] From ref 25. [b] Average distances.

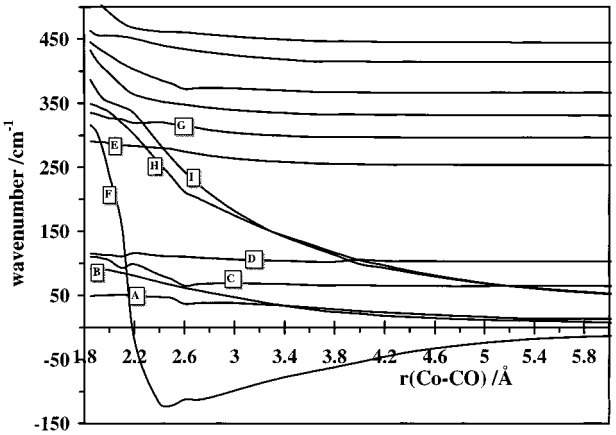

Figure 8. The B3LYP/pvdz calculated frequencies as function of the Co−CO distance. The assignments of the lowest energy vibrational modes are as follows: Cp-rotation (A), OC−Co−CO scissoring (B), out-of-phase wagging of the Cp and the carbonyl planes (C), Cp-wagging in the CO−Co−CO plane (D), in-phase wagging of the Cp and the carbonyl planes (E), Co−CO stretching (F), two combinations of the Cp wagging and a walking motion of the carbonyls (G, H), and the last one below 400 cm^{-1}, the antisymmetric combination of the Co−C−O bending in the OC−Co−CO plane (I).

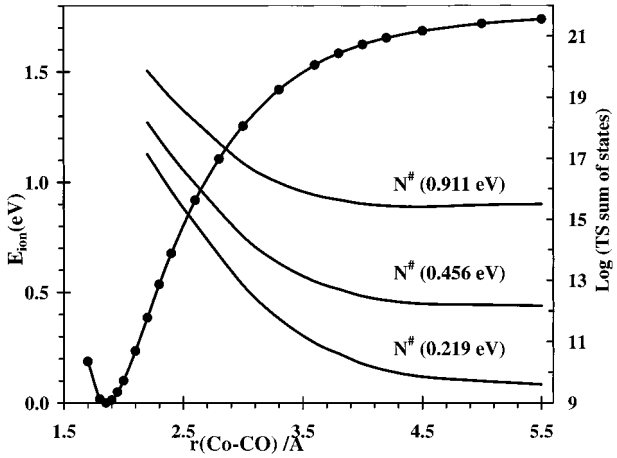

Figure 9. The potential energy curve along the reaction coordinate. The points are the calculated energies at the B3LYP/pvdz level of DFT theory. The calculated sum of states at different energies in excess of the dissociation limit is plotted as a function of the Co−CO bond distance. The three excess energies correspond to photon energies of 9.695, 9.240, and 9.003 eV. Because the calculated dissociation limit of 1.78 eV is higher than the experimental one (1.54 eV), the experimental energy scale is referenced at the dissociation limit.

rates is at low energies, $r = 5.0$ Å was chosen as the Co−CO distance for both the $CpCo(CO)_2^+$ and the $CpCoCO^+$ transition states. The B3LYP/pvdz frequencies calculated with this Co−CO distance were used with a scaling factor of 0.95 as in the case of the ion equilibrium.

It is important to emphasize that the final values of the vibrational frequencies were determined by fitting the data. Although there are 39 frequencies in $CpCo(CO)_2$ and 38 frequencies associated with the transition state, only the four low frequencies in the TS were varied to obtain a fit to the data. This is justified because the RRKM equation is sensitive mainly to the assumed activation energy and the entropy of activation. The latter depends on the difference between the vibrational frequencies of the ion and the TS. As a first approximation, details about individual values are not important. The fitting procedure lowered the three or four frequencies used in the fitting program. This is probably because we emphasized the TOF distribution fits, which are sensitive to the energies very close to the onset where the TS is losest.

Derivation of Thermodynamic Properties. Chipperfield et al.[6] reported a static bomb calorimetry, condensed-phase, heat of formation of cyclopentadienyl−cobalt−dicarbonyl of −169 ± 10 kJ/mol. By combining this with the heat of vaporization obtained from the vapor-pressure measurement, we calculate the gas-phase heat of formation of the complex to be −117 ± 10 kJ/mol. To calculate the 0 K heat of formation, the $H°_{298} - H°_0$ value for $CpCo(CO)_2$ was determined from the calculated vibrational frequencies in Table 1, and the $H°_{298} - H°_0$ values for the elements found in the JANAF tables.[41,42] The latter values are as follows: C, 1.051 kJ/mol; Co, 4.771 kJ/mol; O_2, 8.683 kJ/mol; and H_2, 8.467 kJ/mol. In the thermal contribution of the lowest $CpCo(CO)_2$ frequency (the Cp-ring rotation), a rotational degree of freedom was used instead of a harmonic vibration, because at this temperature it behaves as a hindered rotor with a very low barrier. The calculated $H°_{298} - H°_0$ value for $CpCo(CO)_2$ is 24.18 kJ/mol resulting in a 0 K $\Delta_f H°_0$ of −99 ± 10 kJ/mol.

The 0 K heat of formation of the molecular ion was calculated by adding the adiabatic ionization energy of 7.35 ± 0.01 eV (709.17 kJ/mol) to the neutral $\Delta_f H°_0$, resulting in a 0 K heat of formation of 610 ± 10 kJ/mol. This is shown in Table 3. The $\Delta_f H°_{298}$ [$CpCo(CO)_2^+$] was calculated in the same way as described above but now using the $H°_{298} - H°_0$ value for the ion. Table 3 shows this value to be 596 ± 10 kJ/mol. Consistent with the Rosenstock convention,[15] the heat capacity of the electron was treated as 0.0 kJ/mol at all temperatures. To convert to the JANAF convention,[42] which treats the electron as a chemical element, 6.2 kJ/mol should be added to each ion 298 K heat of formation.

The 0 K $CpCoCO^+$ ion heat of formation was obtained by adding the measured dissociation energy of 12378 cm^{-1} (148

(41) Chase, M. W. *NIST-JANAF Thermochemical Tables*; American Institute of Physics: New York, 1998.

(42) Wagman, D. D.; Evans, W. H. E.; Parker, V. B.; Schum, R. H.; Halow, I.; Mailey, S. M.; Churney, K. L.; Nuttall, R. L. The NBS Tables of Chemical Thermodynamic Properties. In *J. Phys. Chem. Ref. Data Suppl. 2* **1982**, *11*.

Table 3. Auxiliary and Derived Heats of Formation (kJ/mol)[a]

molecule	$\Delta_f H°_{298}$	$\Delta_f {}^{oo}{}_0$	$H°_{298} - H°_0$
$CpCo(CO)_2$	-117 ± 10[b]	-99 ± 10	24.18[c]
$CpCo(CO)_2^+$	596 ± 10[d]	610 ± 10	27.84[c]
$CpCoCO^+$	857 ± 10[d]	872 ± 10	22.24[c]
$CpCo^+$	1113 ± 10[d]	1131 ± 10	17.06[c]
CO	-110.5[e]	-113.8[e]	8.665[e]
Cp•	252.4 ± 11[f]		
Co^+	1185.4 ± 1[g]		
$CpCo^+$	1081 ± 45[h]		

[a] The Rosenstock convention is used for 298 K values for ions in which the electron is assumed to have no internal energy. [b] The condensed phase heat of formation of -169 ± 10 kJ/mol (ref 6) was converted to the gas-phase value using the measured heat of vaporization (see text). [c] Determined in this study from DFT calculations of the vibrational frequencies. [d] From the PEPICO measurements (present work). [e] Wagman et al., ref 42. [f] C_5H_5• EA from McDonald et al.,[44] $C_5H_5^-$ heat of formation from Bartmess et al.[45] [g] JANAF tables.[41] [h] Calculated using the $Cp-Co^+$ bond energy published by Jacobson and Freiser.[43]

kJ/mol) to the 0 K heat of formation of the parent ion and subtracting $\Delta_f H°_{0K}(CO)$. As shown in Table 3, this yields the 0 K heat of formation of 872 kJ/mol and the 298 K value of 857 kJ/mol. The energy barrier of the second CO loss is 12088 cm^{-1} (145 kJ/mol) relative to the $CpCoCO^+$ ion, which leads to a 0 K $CpCo^+$ heat of formation of 1131 kJ/mol and a 298 K value of 1113 kJ/mol.

One of the interesting applications of dissociative photoionization experiments of organometallic complexes such as $CpCo(CO)_2$ is the possibility to dissociate the ion completely as shown in eq 7

$$CpCo(CO)_2 + h\upsilon \rightarrow Co^+ + Cp^{\cdot} + 2CO \qquad (7)$$

If we know the heats of formation of the products, then it is possible to determine the gas-phase heat of formation of the neutral $CpCo(CO)_2$ compound from the 0 K appearance energy of the Co^+ product. Because our hydrogen light source does not produce radiation above about 14 eV, it was not possible for us to measure the energy for reaction 7. However, in a separate experiment, Jacobson and Freiser[43] determined a bond energy for the $Cp-Co^+$ ion of 356 ± 40 kJ/mol on the basis of the $CpCo^+$ ion reactivity with various hydrocarbons. We thus have experimental bond energies for all three bonds in $CpCo(CO)_2^+$ and can determine the heat of formation of the $CpCo(CO)_2$ molecule. The cycle in question and the energies involved in each of the steps are:

$$CpCo(CO)_2 \xrightarrow{713} CpCo(CO)_2^+ \xrightarrow{150} CpCoCO^+ + CO \xrightarrow{145}$$

$$CpCo^+ + 2CO \xrightarrow{356} CO^+ + Cp^{\cdot} + 2CO \qquad (8)$$

The listed 298 K energies are in kJ/mol. The total energy in the complete dissociative photoionization process of eq 8 is thus 1363 kJ/mol. The sum of the product heats of formation is the following: $Co^+(1185.4)$[41] + Cp• (252.4)[44,45] + $2CO(-221)$[42] = 1216.8 kJ/mol. The difference of -146 ± 40 kJ/mol is thus the calculated heat of formation of $CpCo(CO)_2$. This can be compared to our thermochemical value of -117 ± 10 kJ/mol. The discrepancy is just about within the error limits, and thus shows that the overall thermochemistry is correct. Clearly, if a more precise value for the $Cp-Co^+$ value could be obtained, the heat of formation of the parent $CpCo(CO)_2$ molecule could be determined to a greater precision. However, since the dissociative photoionization thermochemical data have a lower error (it is basically determined by the liquid-phase heat of formation), a new and more accurate value for the $Cp-Co^+$ bond energy can be given as 327 ± 15 kJ/mol.

Acknowledgment. We thank the U.S. Department of Energy for a grant for the support of this work. We also acknowledge the North Carolina Supercomputer Center (NCSC) for computer time. This work was also supported by the Hungarian Secretary of Education (grant number FKFP 0162/1999). Bálint Sztáray thanks the ELTE Peregrinatio and the Soros Foundations of Hungary for partial support of his stay in Chapel Hill. Finally, we thank Ms Judit Vaik for the vapor pressure measurements.

JA001077Q

(43) Jacobson, D. B.; Freiser, B. S. *J. Am. Chem. Soc.* **1985**, *107*, 7399−7407.

(44) McDonald, R. N.; Bianchina, E. J.; Tung, C. C. *J. Am. Chem. Soc.* **1991**, *113*, 7115.

(45) Bartmess, J. E.; Scott, J. A.; McIver, R. T., Jr. *J. Am. Chem. Soc.* **1979**, *101*, 6046−6056.